IET Nanobiotechnology

Research Article

IET Journals
The Institution of Engineering and Technology

Optimisation of green synthesis of MnO nanoparticles via utilising response surface methodology

ISSN 1751-8741
Received on 21st July 2017
Revised 19th February 2018
Accepted on 4th March 2018
E-First on 22nd May 2018
doi: 10.1049/iet-nbt.2017.0145
www.ietdl.org

Mahsa Souri[1], Vahid Hoseinpour[1], Alireza Shakeri[1] ✉, Nasser Ghaemi[1]

[1]School of Chemistry, College of Science, University of Tehran, Tehran, Iran

✉ *E-mail: alireza.shakeri@ut.ac.ir*

Abstract: This study concerns the optimisation of green synthesis of manganese oxide nanoparticles (MnO NPs) with *Dittrichia graveolens* (L.) extract via response surface methodology (RSM). Central composite design was used to evaluate the effect of pH, time, and the extract to the metal ratio on the synthesised nanoparticles (NPs). Nine runs were designed to investigate the effect of each parameter while NPs were synthesised under different conditions. Considering the *p*-values (p-value < 0.05), it is indicated that the extract to the metal ratio was the most effective parameter. The synthesised NPs were characterised using UV–vis. Synthesis of the NPs by polyphenolic compounds of green reducing agent and their stabilisation by curcumin was confirmed by Fourier transform infrared spectra and the surface morphology of the spherical MnO NPs was studied by field-emission scanning electron microscopy and transmission electron microscope techniques. The present researchers claimed the optimal condition as follows: time = 56.7 min, pH = 7.2, and the extract to the metal ratio = 87.9 v/v. MnO NPs at optimum condition were then employed for degradation of industrial dyes and they showed high dye degradation activity against Rhodamine B and light green dye. The average size of the synthesised MnO NPs at optimal condition was claimed to be nearly 38 nm.

1 Introduction

Particles with a size up to 100 nm are usually referred as nanoparticles (NPs) [1, 2]. Metal NPs have been extensively studied due to their high specific surface and approved antibacterial and antifungal activities, catalytic, magnetic properties and optical characteristics. Increasing the specific surface area of NP induces their biological effectiveness as a result of an increase in surface energy. Metal oxide NPs are used in generators, vending machines, wrist watches, drug delivery [3] and so on. Nowadays nanotechnology-based products are extensively used in personal-care products, cosmetics, and clothing [4]. Interests in green chemistry have been increased in last few decades in order to eliminate or minimise the waste and utilisation of toxic materials [5, 6]. Green chemistry concerns using non-toxic materials [7], environmentally friendly solvents, and chemicals [8, 9], moreover, it deals with the reduced production of harmful materials [10–12]. NPs can be synthesised through various methods. Typical methods for synthesis of NPs apply toxic chemicals as reducing agents or as stabilising agents to preclude NPs from agglomeration [12]. The noble therapeutic applications of NP oblige using environmentally friendly methods [13]. Using enzymes [14], plant extracts [2], and microorganisms are the biological methods of synthesis of NPs [15].

Synthesis of NPs is to reduce the metal ions in the solution using a reducing agent. NPs are highly reactive due to their high surface energy, and they are aggregated without protection [6]. Lots of natural and synthetic polymers are being used as stabilising agents to prevent metal NPs from sedimentation, agglomeration, and oxidation [16]. Manganese NPs (MnO NPs) are being widely used in wastewater treatment, rechargeable batteries, and sensors of p-nitrophenol, molecular sieve, magnetic materials, and catalysis [17–21].

Dittrichia graveolens (*D. graveolens*) (L.) is a herbaceous plant belonging to Asteraceae family widespread in Mediterranean area [22]. It has been traditionally used as a remedy for cold and wound infection [23] and the biological activities of the extracted plant such as antioxidant [24], antimicrobial [25], and cytotoxic activities [26] have been reported.

Some of the dyes like azo-dyes which are released from industrial processes show high cytotoxic effects on the human and animals [27]. The previous study has shown the ability of green synthesised manganese NPs to degrade Congo red and Safranin O dyes [28]. High surface area of MnO NPs makes them one of the most important environmental friendly catalyst materials [28].

In this approach, distilled water was used as an environmental friendly solvent, and *D. graveolens* (L.) extracts were used as a reducing agent. Curcumin was extracted from turmeric for surface functionalisation of Mn NPs and it was also used as a stabilising agent. Having a wide range of therapeutic effects makes curcumin an important medicinal compound, but because of its low solubility in water, it has low bioavailability. Using curcumin for surface functionalisation of NPs can increase their biological activity [11, 29, 30]. Effective parameters such as time, the ratio of the extracts to the metal and pH were optimised via response surface methodology (RSM) in order to achieve optimal conditions for the synthesis of Mn NPs using *D. graveolens* (L.). Finally, dye degradation activity of MnO NPs is presented.

2 Materials and methods

2.1 Sample preparation

Aerial parts of the *D. graveolens* (L.) were collected from Gorgan, Iran in October and washed using distilled water and then air-dried at room temperature (25°C) under the shad. Then they were ground using an electric grinder.

2.2 Plant extract preparation

10 g of plant materials was boiled in 250 ml distilled water for 2 min. The plant materials were filtered using Whatman no. 1 filter paper and the extracts were centrifuged at 3500 rpm for 15 min and the filtrated extract was dried by evaporating the water with a rotary evaporator. 150 mg of the extract was dissolved in 10 ml distilled water and was stored in an amber bottle, at 10°C until utilisation for the green synthesis of manganese.

For curcumin extraction, 20 g of turmeric was subjected to the Soxhlet apparatus and were extracted with 300 ml of 95% ethanol for 5 h. Turmeric extract was dried at 60°C. 50 mg of the extract

Table 1 Design summary

Factor	Name	Units	Type	Subtype	Min	Max	Coded values	Coded values	Mean	Std. dev.
a	time	min	numeric	continuous	40	120	−1.000 = 40	1.000 = 120	80	34.641
b	pH	—	numeric	continuous	4	8	−1.000 = 4	1.000 = 8	6	1.73205
c	EX	%	numeric	continuous	10	50	−1.000 = 50	1.000 = 90	28.3333	17.5

was dissolved in 10 ml ethanol and stored in an amber bottle, at 10°C until further uses.

2.3 Green synthesis of MnO NPs

Aqueous solutions of manganese acetate (0.01 M) were prepared in different pH values (4–6–8). Nine runs were designed using Design Expert 10. In order to synthesise MnO NPs, the different volumetric ratio of manganese solution and extracts (15 mg/ml) were mixed (extracts/metal: 10:90, 25:75, and 50:50 v/v). The mixtures remained for 40, 80 and 120 min, and then the fresh extract of curcumin (5 mg/ml) was added to the solutions. The samples were centrifuged at 3500 rpm for 15 min. The NPs were separated from the solutions and then washed for several times using ethanol and distilled water.

3 Statistical analysis

A central composite design from RSM was used to evaluate the effect of various factors in the synthesis of the NPs, and to find an optimum condition as well. The three independent variables including times, extracts to the metal ratio, and pH values were studied (Table 1) to find their influence on the synthesis of the NPs. Analysis of variance (ANOVA) was carried out using Design Expert 10 software. In order to illustrate the capability of the models, the coefficient of determination (R^2), and p-values were studied. An insignificant lack of fit and significant model shows the adequacy of the model. The effective factors were represented with a significant p-value (p-value < 0.05).

4 Characterisation of MnO NPs

4.1 UV-vis spectral analysis

The UV–vis spectroscopy is commonly used to characterise different metal NPs in the size range of 2–100 nm [31]. Synthesis of the NP was confirmed by scanning an aqueous solution by UV–vis spectrophotometer at 200–800 nm. All UV–vis spectroscopic measurements of the synthesised MnO NPs were carried out on Perkin Emier, Lambda 25 UV/vis spectrometer.

4.2 Fourier transform infrared (FT-IR) spectrum analysis

Infrared spectra were recorded by FTIR spectroscopy. 1 mg of the synthesised NPs was mixed with 200 mg KBr and was pressed into a pellet. Infrared spectra were recorded using a (Perkin Elmer – Spectrum 65) FT-IR spectroscopy, from 4000 to 400 cm^{-1}.

4.3 Field-emission scanning electron microscopy (FE-SEM)

FE-SEM is a commonly used method for characterisation of the morphology and size of NPs [31]. Microstructural characterisation of the synthesised NPs was done by FE-SEM (HITACHI S-4160).

4.4 TEM (transmission electron microscope)

The TEM was also used for characterisation of the NPs. The resolution of TEM is 1000-fold higher than scanning electron microscopy [32]. The NPs were dispersed in 1 ml of distilled water. A few drops of the solution were placed over the carbon-coated copper grid. After evaporation of the water, TEM measurements were performed using TEM model Philips 30 CM.

4.5 Dye degradation

Light green and Rhodamine B were used to analyse the dye degradation ability of MnO NPs. Dye solutions (50 mg/l) were prepared in distilled water. NPs were dispersed in distilled water (200 µg/ml). Samples containing an equal volume of the dye solution and the NP solution were prepared. The rate of degradation was monitored by measuring the absorbance of the solutions from 400 to 600 nm with a UV–vis spectrophotometer each 5 min.

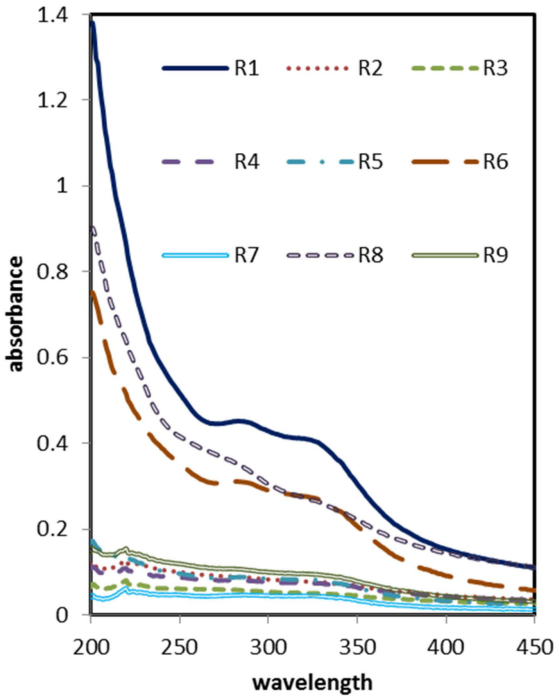

Fig. 1 *UV–vis spectrum of synthesised MnO NPs*

5 Results and discussions

5.1 Experimental design and optimisation

5.1.1 UV–vis spectra studies: The UV–vis absorption intensity of NP depends on NPs concentration which generally increases with the increase of NPs concentration [17] and an increase in the absorption intensity indicates better solubility and dispersion of the NPs in solution [33, 34]. UV–vis spectroscopy of MnO NPs (Fig. 1) shows the maximum absorption at 284 and 325 nm. This is because of $n \rightarrow \pi^*$ transition or $n \rightarrow \pi^*$ and $\pi \rightarrow \pi^*$ transitions. Different place of the absorption bands shows that different morphologies and size variations are presented [35]. Maximal absorption at this wavelength indicates the formation of MnO NPs. Maximal absorptions of MnO NPs at 284 nm have summarised in Table 2. The data were analysed and the polynomial equation was presented in Table 3. ANOVA confirmed that the model is significant. The ratio of the extracts to the metal with p-value < 0.05 was the only effective parameter (Table 3). Insignificant lack of fit and $R^2 = 0.8354$ indicate the propriety of the model (Table 3). The effect of each parameter is shown in Fig. 2. The results marks that the most effective parameter was the ratio of the extracts to the metal and Fig. 2 illustrates that the higher ratio of the extract to the metal causes the synthesis of NPs to increase while increasing the time and decreasing the pH provides a minor positive effect. The intensity of the band is seen to be a function of the amount of *D. graveolens* extract used in the reaction and the increase in the extracts concentration led to an increase in the synthesis of MnO NPs. According to Kumar *et al.* [21] most of the MnO NPs were synthesised in 30 min and further time did not affect the reaction.

Table 2 Maximal absorption of Mn NPs at 284 nm

Std[a]	Run	Factor 1 A: time min	Factor 2 B: pH	Factor 3 C: Ex %	Response 1 absorption
3	1	40	4	50	0.4515
5	2	40	6	25	0.0981
2	3	40	8	10	0.0579
7	4	80	4	25	0.0799
6	5	80	6	10	0.0463
1	6	80	8	50	0.3099
4	7	120	4	10	0.046
9	8	120	6	50	0.573
8	9	120	8	25	0.1068

[a]Standard order.

Table 3 Analyse of variance

Source	Sum of squares	df[a]	Mean square	Value	*p*-value Prob > *F*	
model	0.26	3	0.088	8.46	0.0210	significant
a-time	2.332×10^{-3}	1	2.332×10^{-3}	0.22	0.6555	—
b-pH	1.761×10^{-3}	1	1.761×10^{-3}	0.17	0.6975	—
c-EX	0.26	1	0.26	24.99	0.0041	significant
residual	0.052	5	0.010	—	—	—
cor total	0.32	8	—	—	—	—

[a]Degree of freedom.

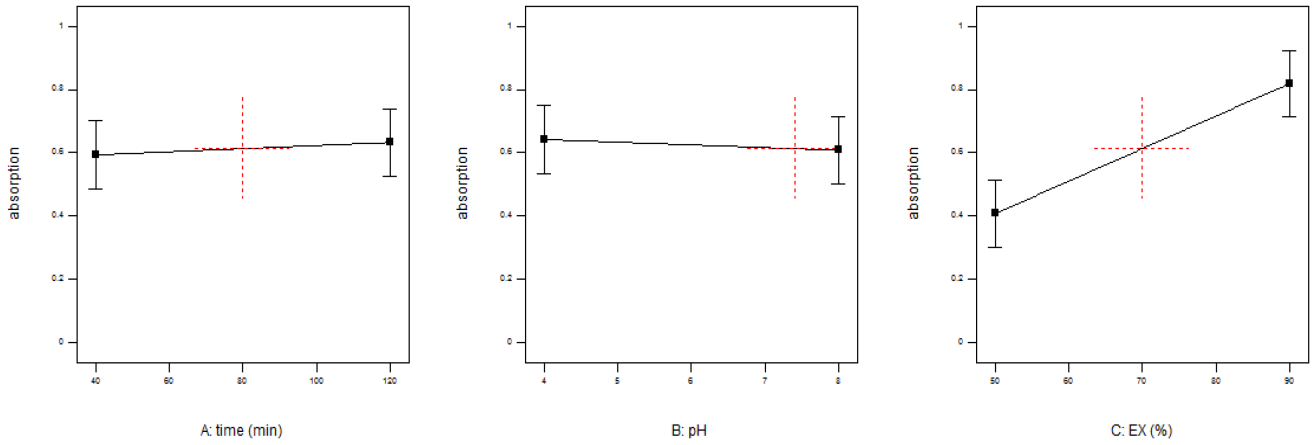

Fig. 2 *Effect of factors on synthesise of NPs*

Polynomial equations summarised the influence of each factor, and it can be found considering the sign and magnitude of each parameter, e.g. (1) is the final equation in terms of coded and actual factors represented in, e.g. (2).

$$\text{Absorption} = 0.625324 + 0.0197167 * A + (-0.0171333 * B) + 0.205788 * C \quad (1)$$

$$\text{Absorption} = -0.082966 + 0.000492917 * \text{time} + (-0.00856667 * \text{pH}) + 0.0102894 * \text{EX} \quad (2)$$

5.1.2 Optimisation of synthesis of MnO NPs: The normal plot that is shown in Fig. 3*d* indicates the normality of the data and the response surface plots shown in Figs. 3*a–c* give information about the significance of factor *C*. Figs. 3*a* and *b* indicate that the increase in the concentration of the extract increases the synthesis of MnO NPs while the increase in pH and time did not change the result significantly (Fig. 3*c*). The optimum condition for the synthesis of MnO NP was found to be as follows: time = 56.7 min, pH = 7.2, and Ex% = 87.9 v/v in order to obtain maximal absorption 0.787.

5.2 Characterisation of MnO NPs

5.2.1 UV–vis spectral analysis: Fig. 4 indicates the UV–vis plot of MnO NPs stabilised by curcumin in optimum condition. Maximal absorption at 240 nm indicates the presence of MnO NPs which are stabilised by curcumin.

5.2.2 FT-IR studies: It has been reported in the literature that plant constituents play a key role in the reduction of metal ions [36, 37]. FT-IR spectroscopy was used to identify the responsible functional group existing in the biomolecules of the *D. graveolens* extract to reduce the manganese ions.

FT-IR spectra of turmeric and *D. graveolens* extract are shown in Fig. 5. A spectrum of the MnO NPs is shown in Fig. 5*c*. The broad peak at 3420 cm^{-1} corresponds to an O–H band stretching vibration presence in the system [11]. Peaks around 470, 509, 700 and 798 cm^{-1} were due to MnO NPs [21, 38]. The peak at 2917 cm $^{-1}$ relates to –C = C bond, 1500–1560 cm^{-1} peaks relate to the aromatic C = C bond of curcumin system which surrounds the NPs and prevents them from agglomeration. The C = O bond of curcumin appears at 1650 cm^{-1}. The C–O band of curcumin was assigned by the peak at 1030 cm^{-1}. FT-IR spectra of the extracts (Figs. 5*a* and *b*) also show the OH bending modes of the phenolic compounds of the extracts which are responsible for the reduction

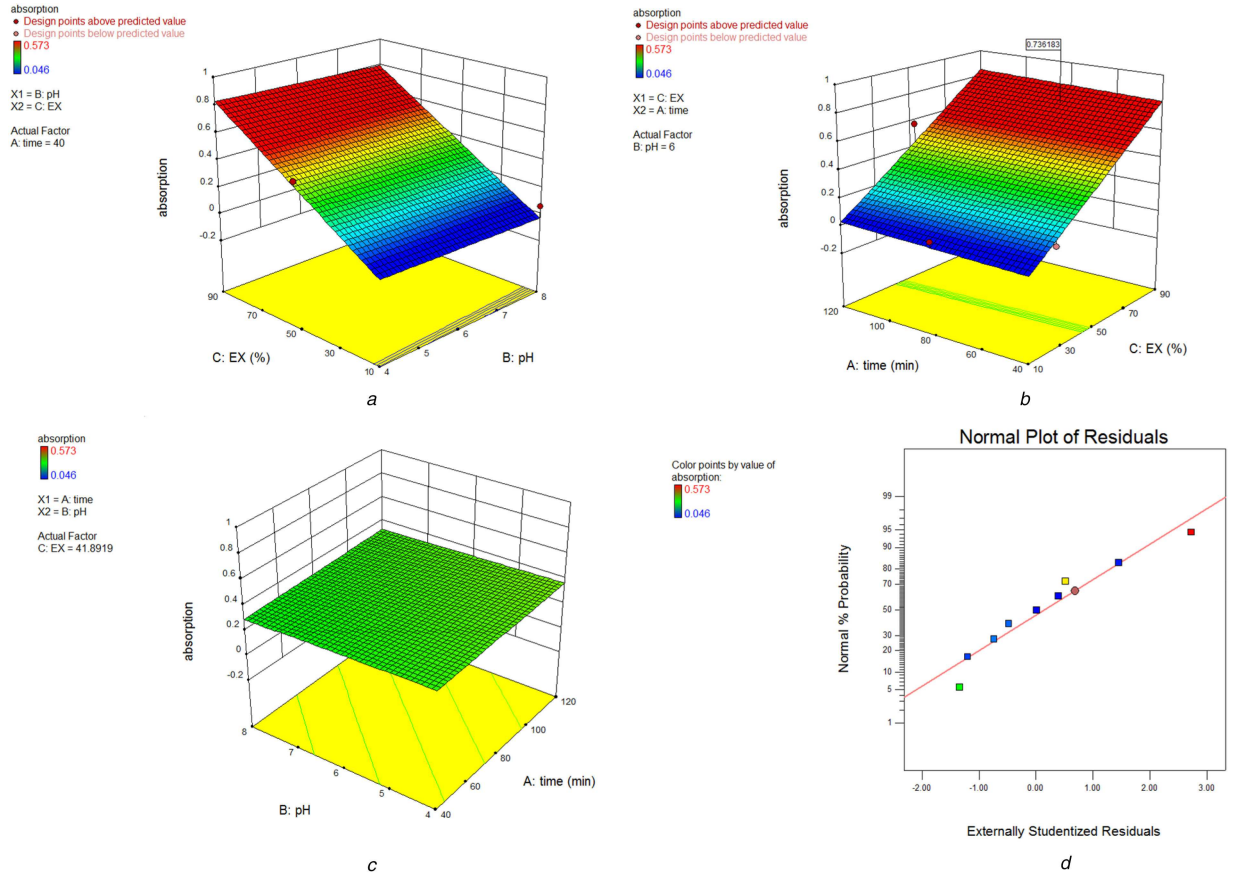

Fig. 3 *3D plot showing the effect of*
(a) pH and Ex, ***(b)*** Ex and time, ***(c)*** pH and time, ***(d)*** On absorbance and normal plot

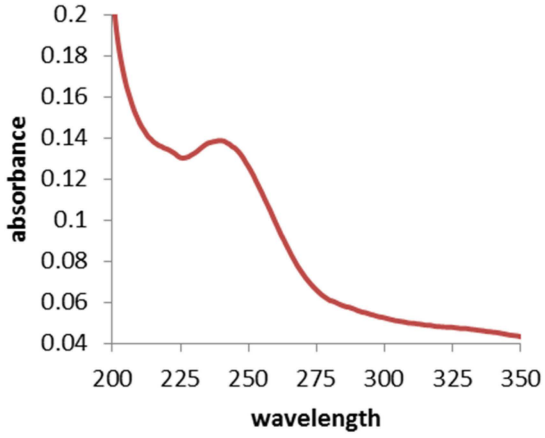

Fig. 4 *UV–vis spectrum of MnO NPs in optimum condition*

of ions and peaks at 1500–1700 relate to C = C bands of aromatic rings of phenolic compounds.

Comparison of the spectra of the extracts and MnO NPs indicates the effect of the extracts in the synthesis of the NPs.

5.2.3 FE-SEM and TEM studies: FE-SEM images of MnO NPs at optimum condition were shown in Fig. 6. It is shown that spherical NPs are formed with an average diameter of 38 nm. These results illustrate the formation of MnO NPs using reduction agent (*D. graveolens* extracts).

The morphology and structure of the MnO NPs at higher resolution are shown in the TEM images (Fig. 7). The images obviously indicate the presence of secondary material capping NPs which assigned to bioorganic compounds that synthesised and stabilised the spherical MnO NPs [39–41].

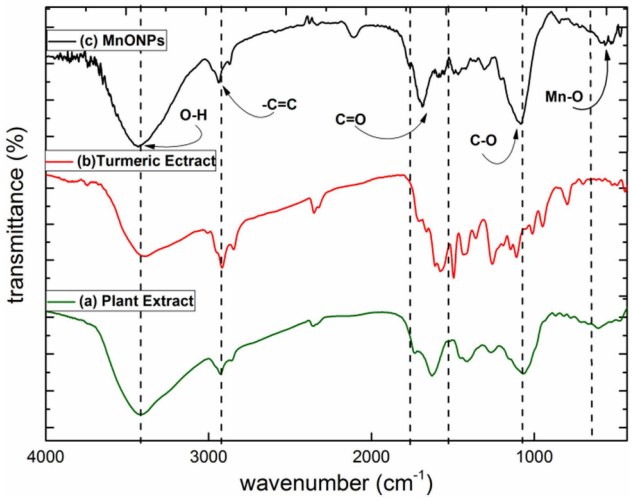

Fig. 5 *FT-IR spectrum of*
(a) *D. graveolens* extract, ***(b)*** Turmeric extract, ***(c)*** MnO NPs

5.3 Dye degradation

The kinetics of light green and Rhodamine B degradation using MnO NPs were monitored using UV–vis spectroscopy. Fig. 8*a* shows the UV–vis spectra of the decomposition of the light green over the variation of the time from 0 to 17 min; in addition, a decreasing of absorbance at a maximum wavelength of 625 nm is observed. Light green id degraded almost completely in 17 min. Fig. 8*b* illustrates UV–vis spectra of decomposed Rhodamine B dye at different periods of time from 0 to 22 min and shows the maximum absorption wavelength at 540 nm. Absorbance intensities of the Rhodamine B solutions are decreased by the presence of MnO NPs over the variation of the time. Rhodamine B dye is degraded almost completely in 22 min.

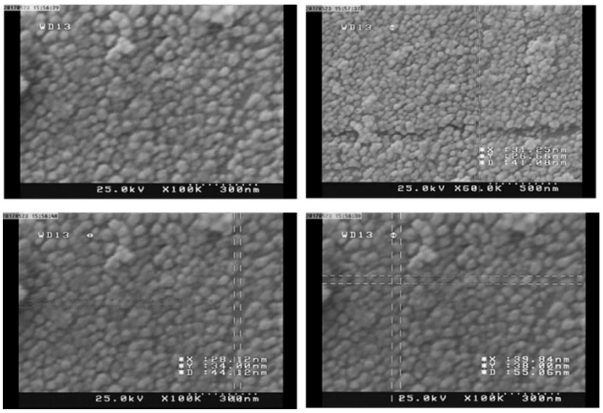

Fig. 6 *FE-SEM characterisation of MnO NPs*

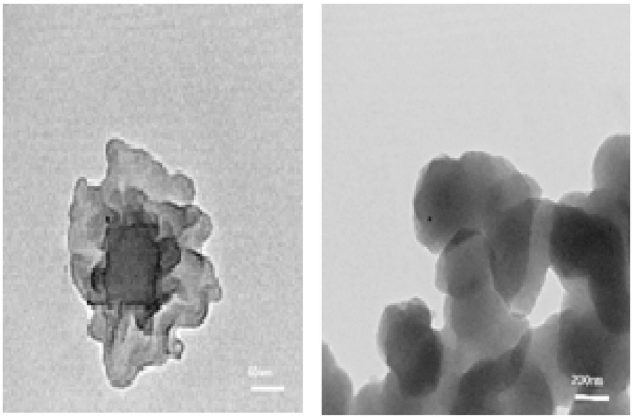

Fig. 7 *TEM images of MnO NPs*

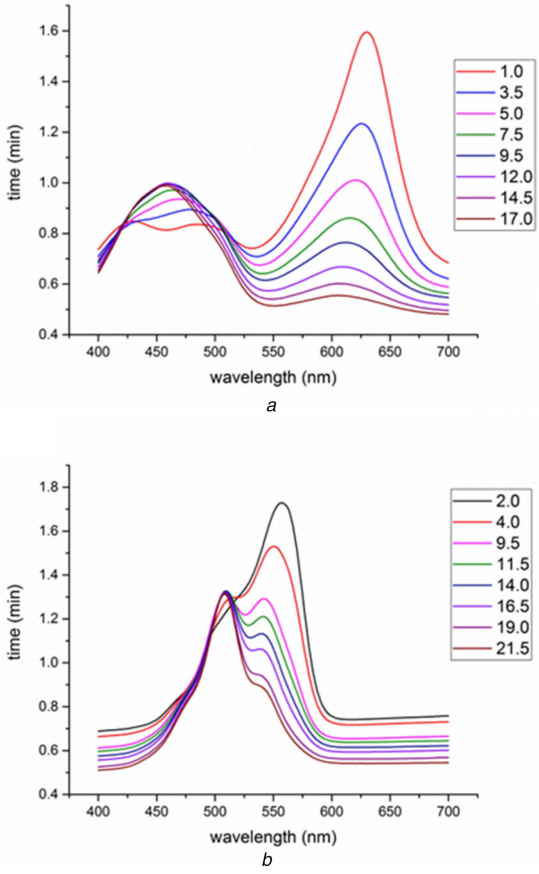

Fig. 8 *Dye degradation of*
(a) Light green and, ***(b)*** Rhodamine B using MnO NPs with time

6 Conclusions

In this study, MnO NPs were synthesised using *D. graveolens* extract. This method is green, fast and economical. This study was carried out to optimise the synthesis of MnO NPs by using RSM. The parameters of enhancement including time, the extract to the metal ratio and pH were observed. The results indicate that the increase in the concentration of the extract increases the synthesis of MnO NPs while the increase in pH and time did not change the result significantly. The morphological study of the synthesised MnO NPs with FE-SEM and TEM revealed that the NPs were spherical with an average size of 38 nm. FTIR spectra illustrate the effect of plant extracts in the extraction of NPs. The dye degradation activity of the synthesised NPs was carried out by performing the decomposition of Rhodamine B and light green dyes by adding the synthesised MnO NPs which showed that the absorbance of the dye decreased after 20 min.

7 References

[1] Makkar, H.P., Blümmel, M., Borowy, N.K., *et al.*: 'Gravimetric determination of tannins and their correlations with chemical and protein precipitation methods', *J. Sci. Food Agric.*, 1993, **61**, (2), pp. 161–165

[2] Bakkali, F., Averbeck, S., Averbeck, D., *et al.*: 'Biological effects of essential oils–a review', *Food Chem. Toxicol.*, 2008, **46**, (2), pp. 446–475

[3] Treutter, D.: 'Significance of flavonoids in plant resistance: a review', *Environ. Chem. Lett.*, 2006, **4**, (3), p. 147

[4] Handa, S.S., Khanuja, S.P.S., Longo, G., *et al.*: '*Extraction technologies for medicinal and aromatic plants*' (Trieste (Italy): Earth, Environmental and Marine Sciences and Technologies, 2008)

[5] Nerio, L.S., Olivero-Verbel, J., Stashenko, E.: 'Repellent activity of essential oils: a review', *Bioresour. Technol.*, 2010, **101**, (1), pp. 372–378

[6] González-Coloma, A., Martín-Benito, D., Mohamed, N., *et al.*: 'Antifeedant effects and chemical composition of essential oils from different populations of *Lavandula luisieri* L', *Biochem. Syst. Ecol.*, 2006, **34**, (8), pp. 609–616

[7] Haseeb, M.T., Hussain, M.A., Abbas, K., *et al.*: 'Linseed hydrogel-mediated green synthesis of silver nanoparticles for antimicrobial and wound-dressing applications', *Int. J. Nanomed.*, 2017, **12**, p. 2845

[8] Vishwasrao, C., Momin, B., Ananthanarayan, L.: 'Green synthesis of silver nanoparticles using sapota fruit waste and evaluation of their antimicrobial activity', *Waste Biomass Valorization*, 2018, pp. 1–11

[9] Hussain, M.A., Shah, A., Jantan, I., *et al.*: 'One pot light assisted green synthesis, storage and antimicrobial activity of dextran stabilized silver nanoparticles', *J. Nanobiotechnol.*, 2014, **12**, (1), p. 53

[10] Savelev, S., Okello, E., Perry, N., *et al.*: 'Synergistic and antagonistic interactions of anticholinesterase terpenoids in *Salvia lavandulaefolia* essential oil', *Pharmacol. Biochem. Behav.*, 2003, **75**, (3), pp. 661–668

[11] Savelev, S.U., Okello, E.J., Perry, E.K.: 'Butyryl-and acetyl-cholinesterase inhibitory activities in essential oils of salvia species and their constituents', *Phytother. Res.*, 2004, **18**, (4), pp. 315–324

[12] Azwanida, N.: 'A review on the extraction methods use in medicinal plants, principle, strength and limitation', *Med. Aromat Plants*, 2015, **4**, pp. 196, doi: 2167–0412.1000196

[13] Miguel, M.G.: 'Antioxidant and anti-inflammatory activities of essential oils: a short review', *Molecules*, 2010, **15**, (12), pp. 9252–9287

[14] Burt, S.: 'Essential oils: their antibacterial properties and potential applications in foods – a review', *Int. J. Food Microbiol.*, 2004, **94**, (3), pp. 223–253

[15] Kumar, R., Tripathi, Y.: 'Getting fragrance from plants', '*Training manual on extraction technology of natural dyes & aroma therapy and cultivation value addition of medicinal plants*' (Forest Research Institute, Dehradun, Indian, 2011, 1 edn.), pp. 77–102

[16] Kaufmann, B., Christen, P.: 'Recent extraction techniques for natural products: microwave-assisted extraction and pressurised solvent extraction', *Phytochem. Anal.*, 2002, **13**, (2), pp. 105–113

[17] Steffen, L.M.: 'Eat your fruit and vegetables', *Lancet*, 2006, **367**, (9507), pp. 278–279

[18] Hagerman, A.E., Butler, L.G.: 'Choosing appropriate methods and standards for assaying tannin', *J. Chem. Ecol.*, 1989, **15**, (6), pp. 1795–1810

[19] Becker, K., Makkar, H.P., Siddhuraju, P., *et al.*: '*Plant secondary metabolites*', (Springer, Humana Press, 2007), pp. 1–3

[20] Hagerman, A.E., Butler, L.G.: 'Protein precipitation method for the quantitative determination of tannins', *J. Agric. Food Chem.*, 1978, **26**, (4), pp. 809–812

[21] Kumar, V., Singh, K., Panwar, S., *et al.*: 'Green synthesis of manganese oxide nanoparticles for the electrochemical sensing of P-nitrophenol', *Int. Nano Lett.*, 2017, **7**, (2), pp. 123–131

[22] Blanc, M.C., Muselli, A., Bradesi, P., *et al.*: 'Chemical composition and variability of the essential oil of *Inula graveolens* from Corsica', *Flavour Fragrance J.*, 2004, **19**, (4), pp. 314–319

[23] Pieroni, A., Giusti, M.E., De Pasquale, C., *et al.*: 'Circum-Mediterranean cultural heritage and medicinal plant uses in traditional animal healthcare: a field survey in eight selected areas within the RUBIA project', *J. Ethnobiol. Ethnomed.*, 2006, **2**, (1), p. 1

[24] Giamperi, L., Bucchini, A., Cara, P., *et al.*: 'Composition and antioxidant activity of *Nepeta foliosa* essential oil from Sardinia (Italy)', *Chem. Nat. Compd.*, 2009, **45**, (4), pp. 554–556

[25] Mitic, V., Jovanovic, V.S., Ilic, M.*, et al.*: '*Dittrichia graveolens* (L.) Greuter essential oil: chemical composition, multivariate analysis, and antimicrobial activity', *Chem. Biodivers.*, 2016, **13**, (1), pp. 85–90
[26] Topcu, G., Oksuz, S., Shieh, H.L.*, et al.*: 'Cytotoxic and antibacterial sesquiterpenes from *Inula-graveolens*', *Phytochemistry*, 1993, **33**, (2), pp. 407–410
[27] Nony, C.R., Bowman, M.C., Cairns, T.*, et al.*: 'Metabolism studies of an azo dye and pigment in the hamster based on analysis of the urine for potentially carcinogenic aromatic amine metabolites', *J. Anal. Toxicol.*, 1980, **4**, (3), pp. 132–140
[28] Moon, S.A., Salunke, B.K., Alkotaini, B.*, et al.*: 'Biological synthesis of manganese dioxide nanoparticles by *Kalopanax pictus* plant extract', *IET Nanobiotechnol.*, 2015, **9**, (4), pp. 220–225
[29] Haslam, E.: '*Vegetable tannins. Biochemistry of plant phenolics*' (Springer, US, 1979), pp. 475–523
[30] Hagerman, A.E., Butler, L.G.: 'The specificity of proanthocyanidin-protein interactions', *J. Biol. Chem.*, 1981, **256**, (9), pp. 4494–4497
[31] Mittal, A.K., Chisti, Y., Banerjee, U.C.: 'Synthesis of metallic nanoparticles using plant extracts', *Biotechnol. Adv.*, 2013, **31**, (2), pp. 346–356
[32] Eppler, A.S., Rupprechter, G., Anderson, E.A.*, et al.*: 'Thermal and chemical stability and adhesion strength of Pt nanoparticle arrays supported on silica studied by transmission electron microscopy and atomic force microscopy', *J. Phys. Chem. B*, 2000, **104**, (31), pp. 7286–7292
[33] Rathi, B., Bodhankar, S., Baheti, A.: 'Evaluation of aqueous leaves extract of *Moringa oleifera* Linn for wound healing in albino rats', 2006
[34] De Castro, M.L., Garcıa-Ayuso, L.: 'Soxhlet extraction of solid materials: an outdated technique with a promising innovative future', *Anal. Chim. Acta*, 1998, **369**, (1), pp. 1–10
[35] Trusheva, B., Trunkova, D., Bankova, V.: 'Different extraction methods of biologically active components from propolis: a preliminary study', *Chem. Cent. J.*, 2007, **1**, (1), p. 13
[36] Rajakumar, G., Rahuman, A.A., Priyamvada, B.*, et al.*: '*Eclipta prostrata* leaf aqueous extract mediated synthesis of titanium dioxide nanoparticles', *Mater. Lett.*, 2012, **68**, pp. 115–117
[37] Muzaffar, S., Tahir, H.: 'Enhanced synthesis of silver nanoparticles by combination of plants extract and starch for the removal of cationic dye from simulated waste water using response surface methodology', *J. Mol. Liq.*, 2018, **252**, pp. 368–382
[38] Ranitha, M., Nour, A.H., Ziad, A.*, et al.*: 'Optimization of microwave assisted hydrodistillation of Lemongrass (*Cymbopogon citratus*) using response surface methodology', *Int. J. Res. Eng. Technol.*, 2014, **3**, pp. 5–14
[39] Sangeetha, G., Rajeshwari, S., Venckatesh, R.: 'Green synthesis of zinc oxide nanoparticles by *Aloe barbadensis* miller leaf extract: structure and optical properties', *Mater. Res. Bull.*, 2011, **46**, (12), pp. 2560–2566
[40] Huang, J., Li, Q., Sun, D.*, et al.*: 'Biosynthesis of silver and gold nanoparticles by novel sundried *Cinnamomum camphora* leaf', *Nanotechnology*, 2007, **18**, (10), p. 105104
[41] Wang, M., Na, E.K., Kim, J.S.*, et al.*: 'Photoluminescence of ZnO nanoparticles prepared by a low-temperature colloidal chemistry method', *Mater. Lett.*, 2007, **61**, (19), pp. 4094–4096